Electrochemical synthesis and structural characterization of Co(II), Ni(II) and Cu(II) complexes of *N,N*-bis(4,5-dimethyl-2-hydroxybenzyl)-*N*-(2-pyridylmethyl)amine†

Elena Labisbal,[a] Laura Rodríguez,[a] Oscar Souto,[a] Antonio Sousa-Pedrares,[a] José Arturo García-Vázquez,*[a] Jaime Romero,[a] Antonio Sousa,[a] Matilde Yáñez,[b] Francisco Orallo[b] and José A. Real[c]

Received 16th April 2009, Accepted 4th August 2009
First published as an Advance Article on the web 24th August 2009
DOI: 10.1039/b907539a

The electrochemical oxidation of anodic metal (cobalt, nickel or copper) in a cell containing an acetonitrile solution of the ligand *N,N*-bis(4,5-dimethyl-2-hydroxybenzyl)-*N*-(2-pyridylmethyl)amine (H_2L) affords complexes $[Co_2L_2]\cdot H_2O$ (**1**), $[Ni_3L_3]$ (**2**) and $[Cu_2L_2]$ $3H_2O$ (**4**). On using nickel as the anode and the addition to the solution electrolytic phase of the amount of water necessary to saturate the solution, the electrolytic process gave rise to the new compound $[Ni_2L_2(H_2O)_{1.5}]\cdot CH_3CN$ (**3**). Compounds **1** and **4** are dimeric and the metal atoms are pentacoordinated. Compound **3** also consists of dimeric neutral molecules with the nickel atoms in both penta- and hexacoordinated environments. The crystal structure of **2** shows the presence of a trimeric compound in which the nickel atoms are hexacoordinated. Electronic, IR and FAB spectra of the complexes are discussed and related to the structural information. The magnetic behavior of **1–4** denotes the occurrence of intramolecular antiferromagnetic interactions. The values obtained for the coupling constant J are -4.2 cm^{-1}, -5.3 cm^{-1}, -30 cm^{-1} and -4.7 cm^{-1} for **1**, **2**, **3** and **4**, respectively. These values are in full agreement with the structural characteristics of the compounds. The catalytic activity of the complexes towards the decomposition of hydrogen peroxide (catalase activity) was also studied.

Introduction

Much of the interest in transition metal complexes of chelating alkoxide and aryl-oxide ligands results from their potential relevance as catalytic systems for the polymerization of alpha-olefins.[1] A substantial amount of work has been carried out with monodentate phenolate[2,3] and chelating phenolate[4–6] ligands, mainly on group IV and V metals. Dianionic amine bis(phenolate) ligands were recently used as an approach to increase the hydrophobic nature of the coordinating ligands.[7] However, the use of chelating phenolates in other transition-metal groups is still rare.[8,9] In addition, interest in the structure and reactivity of transition metal complexes with this type of ligand is related, in part, to the fact that they can be used as mimetic small molecular models for the active sites of several redox and hydrolytic enzymes.[10–14]

The ability of aryl-oxide functionalized ligands to facilitate efficiently the magnetic coupling between two paramagnetic metal ions represents another source of interest in the realm of molecular magnetism.[15,16] Indeed, dinucleating ligands that contain a potentially bridging phenoxo oxygen and nitrogen donor sets have been widely used in the synthesis of dinuclear complexes of copper,[17] manganese,[18] cobalt,[19] iron[20] and zinc.[19] As in hydroxo- and alkoxo-bridged metal complexes, the nature of the magnetic interactions in phenoxo-bridged metal systems is primarily determined by the M–O–M angle and the M···M separation.[21,22]

As part of our research in this area, we report here the preparation, structure determination, magnetic properties and "catalase-like" activities of cobalt, nickel and copper complexes of the sterically hindered tripodal ligand *N,N*-bis(4,5-dimethyl-2-hydroxybenzyl)-*N*-(2-pyridylmethyl)amine [H_2L]) (Scheme 1).

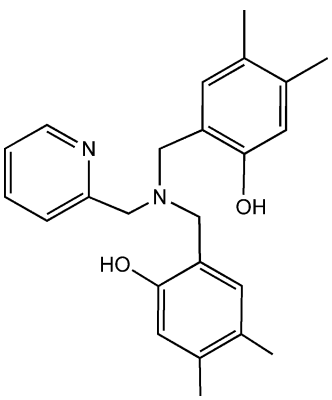

Scheme 1

[a]*Departamento de Química Inorgánica, Universidad de Santiago de Compostela, 15782, Santiago de Compostela, Spain. E-mail: josearturo.garcia@usc.es; Fax: +34-(9)81547102; Tel: +34-(9)81 563100, ext. 14950*
[b]*Departamento de Farmacología, Universidad de Santiago de Compostela, 15782, Santiago de Compostela, Spain*
[c]*Institut de Ciencia Molecular/Departamento de Química Inorgánica, Universitat de Valencia, 46071, Valencia, Spain*

† Electronic supplementary information (ESI) available: The crystal parameters, experimental details for data collection and bond distances and angles for **1–4** compounds. CCDC reference numbers 710317–710320. For ESI and crystallographic data in CIF or other electronic format see DOI: 10.1039/b907539a

Experimental

General considerations

All solvents, 3,4-dimethylphenol, 2-(2-aminomethyl)pyridine and 37% aq. formaldehyde were commercial products (Aldrich) and were used as supplied. Cobalt, nickel and copper (Ega Chemie) were used as plates (*ca.* 2 × 2 cm). The chemicals used in the catalase-like properties experiments were the tested compounds, catalase from bovine liver and dimethylsulfoxide (purchased from Sigma-Aldrich), resorufin sodium salt, H_2O_2, sodium phosphate and HRP (supplied in the Amplex® Red MAO assay kit from Molecular Probes, Inc., Eugene, Oregon, USA). Appropriate dilutions of the above substances were prepared every day immediately before use in deionized water from the following concentrated stock solutions kept at −20 °C: test compounds (0.1 M) in DMSO; resorufin, H_2O_2 and HRP (0.1 M) in deionized water. Due to the photosensitivity of some chemicals (*e.g.*, Amplex® Red reagent), all experiments in which these compounds were used were performed in the dark. In all assays, neither deionized water (Milli-Q®, Millipore Ibérica S.A., Madrid, Spain) nor appropriate dilutions of the vehicle used (DMSO) had significant pharmacological effects.

Physical measurements

Elemental analyses were performed using Carlo-Erba EA 1112 and Carlo-Erba EA 1108 microanalysers. IR spectra were recorded on KBr discs using a Bruker IFS 66V spectrophotometer and an ABB Bomen 102 spectrophotometer. ^{1}H and ^{13}C NMR spectra were recorded on Bruker AMX350 MHz and Bruker AC-300 instruments using $CDCl_3$ as solvent and chemical shifts were determined against TMS. Electrospray mass spectral data were obtained with 5×10^{-4} M solutions (MeOH or CMe_2Cl_2) by flow injection into a Hewlett-Packard 1100 series MSD. The carrier solvent was 49% MeOH/49% H_2O/2% formic acid or 98% CH_2Cl_2/2% formic acid. Electrospray ionization conditions were as follows: nitrogen drying gas flow 10.0 L min^{-1}; nebulizer pressure, 40 psig; drying gas temperature 350 °C; capillary voltage, 4 kV. The capillary exit voltage was varied from 0 to 150 V. Variable temperature magnetic susceptibility measurements were carried out using microcrystalline samples (20–60 mg) of compounds **1–4**, using a Quantum Design MPMS2 SQUID susceptometer equipped with a 5.5 T magnet, operating at 0.1–0.5 T and at temperatures from 300–1.8 K. The susceptometer was calibrated with $(NH_4)_2Mn(SO_4)_2 \cdot 12H_2O$. Experimental susceptibilities were corrected for diamagnetism of the constituent atoms by the use of Pascal's constants.

Potential catalase-like properties of the synthesized compounds were evaluated under physiological conditions, *i.e.*, in aqueous solution at pH = 7.2–7.4 and at micromolar concentrations of the catalyst and hydrogen peroxide (H_2O_2). The assay procedure was performed at 37 °C in a total volume of 1 mL containing 50 mM sodium phosphate buffer, 100 μM H_2O_2 and the appropriate amount of the tested compounds. At different time intervals, aliquots of the reaction mixture were suitably diluted (1/100) in sodium phosphate buffer and the remaining H_2O_2 present in these diluted aliquots was quantified by the Amplex® Red–Hydrogen Peroxide method.[23,24] This is a fluorescence assay in which the Amplex® Red reagent (10-acetyl-3,7-dihydroxyphenoxazine) reacts (with a stoichometry of 1:1) with H_2O_2 in the presence of HRP to produce the highly fluorescent oxidation product, resorufin.

To measure H_2O_2, equal volumes of sample and Amplex® Red-HRP working solution were mixed. The final reaction mixture contained 50 μM Amplex® Red reagent and 0.1 units (U)/mL HRP. After 10 min, the amount of resorufin generated was quantified in a fluorescent plate reader (FLx800, Bio-Tek Instruments, Inc., Winooski, Vermont, USA), using excitation at 545 nm with emission detection at 590 nm. Fluorescence was converted to H_2O_2 concentration by using a curve generated from standard samples containing known amounts of H_2O_2. The assay was linear in the range from 0 to 5 μM H_2O_2. Control experiments were carried out simultaneously by replacing the tested compounds with appropriate dilutions of the vehicles. In addition, the possible ability of the tested complexes to modify the fluorescence generated in the reaction mixture due to non-enzymatic inhibition (*e.g.*, by direct reaction with Amplex® Red reagent) was determined by adding these complexes to solutions containing only the Amplex® Red reagent in a sodium phosphate buffer.

For details of data presentation and statistical analysis see the ESI.†

Ligand synthesis

The ligand H_2L was prepared by the one-pot Mannich condensation[25,26] between 3,4-dimethylphenol (6.11 g, 50 mmol), formaldehyde 37% (51.4 mL, 50 mmol) and 2-(aminomethyl)pyridine (22.6 mL, 25 mmol) in ethanol as solvent. The reaction mixture was refluxed during 6 h and then cooled. The resulting white solid was filtered off, washed with water and crystallized from dichloromethane (8.75 g, 93%). ^{1}H NMR (350 Mz, $CDCl_3$, 25 °C, TMS, ppm): δ = 8.64, 7.70 and 7.14 (1H, pyridine ring); 6.79 and 6.69 (s, 2H, phenyl); 3.86 (s, 2H, -CH_2-py); 3.74 (s, 4H, -CH_2-); 2.17 and 2.74 (s, 6H, -CH_3). ^{13}C NMR (300 Mz, 25 °C, TMS, $CDCl_3$, ppm) δ 152 (*C*–OH); 137.8–118.4 (C-aromatic); 56.1 (N–*C*H_2), 55.7 (N–*C*H_2, py) 19.8–18.9 (-*C*H_3); IR (KBr) ν = 1002(vs), 1241(s), 1294(s), 1504(vs), 1597(vs), 1630(s), 3100–3350(vbr) cm^{-1}; EI MS *m*/*z* 377.4 (M^+): elemental analysis calcd (%) for $C_{24}H_{28}N_2O_2$: C 76.5, H, 7.4, N, 7.5; found: C 76.6, H 7.5, N 7.4.

Electrochemical synthesis of the metal complexes

The complexes were obtained using an electrochemical procedure (Scheme 2).[27] The cell consisted of a tall-form beaker (100 mL) fitted with a rubber bung through which the electrochemical leads entered. An acetonitrile solution of the ligand, containing a few mg of tetramethylammonium perchlorate as a current carrier, was electrolyzed using a platinum wire as the cathode and a metal plate as the sacrificial anode (**Caution:** *Although problems were not encountered in this work, all perchlorate compounds are potentially explosive, and should be handled in small quantities and with great care!*). The applied voltages (10–20 V) allowed sufficient current flow for smooth dissolution of the metal. The current was maintained at 5 mA for 1 h. In all cases, during the electrolysis hydrogen was evolved at the cathode. Under these conditions the cell can be summarized as $M_{(+)}/H_2L + CH_3CN/Pt_{(-)}$.

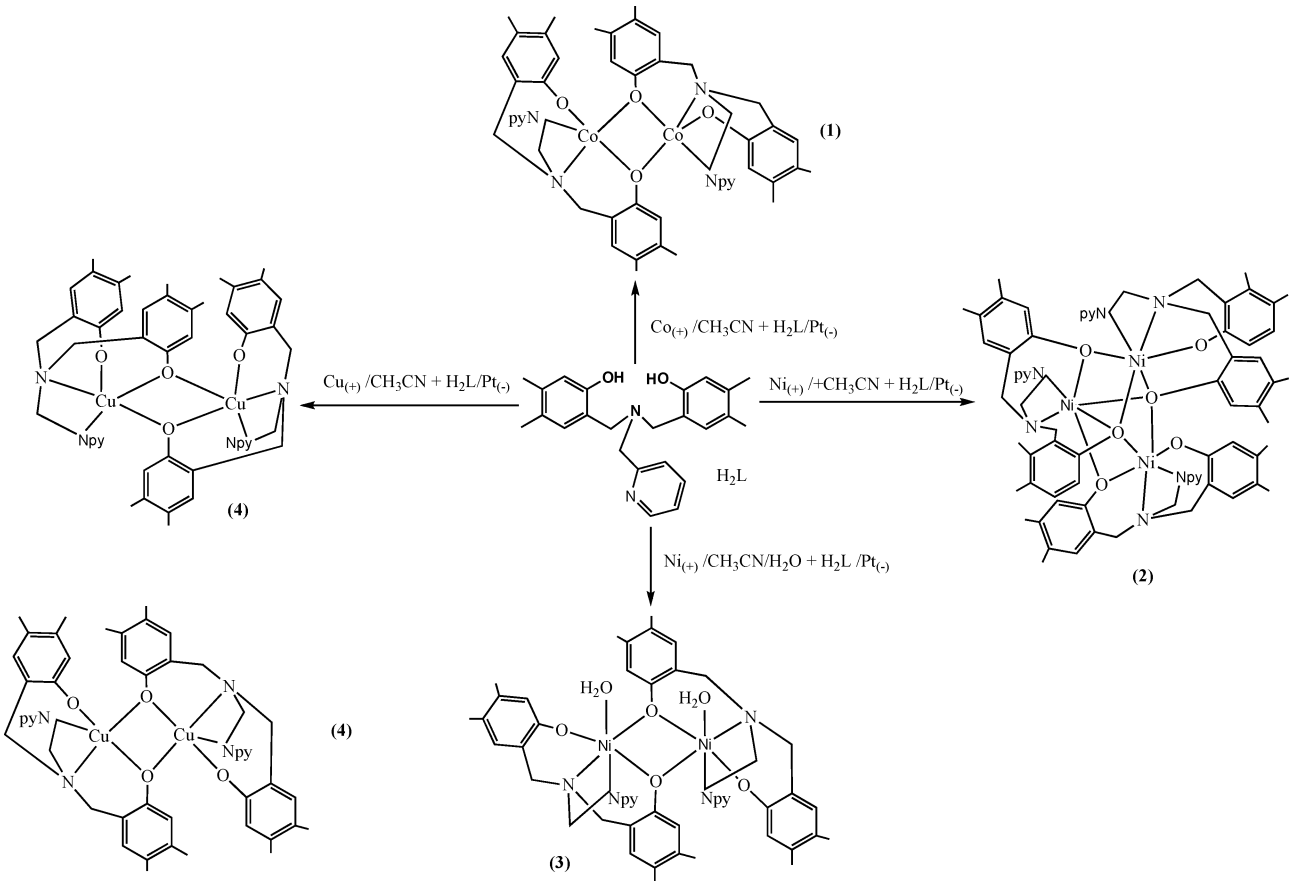

Scheme 2 Schematic representation of the electrochemical synthesis of complexes.

Synthesis of $[Co_2L_2]\cdot H_2O$(1). Electrochemical oxidation of a cobalt anode in a solution of H_2L (0.035 g, 0.093 mmol) in acetonitrile (80 cm^3) at 10 V and 5 mA for 1 h caused 5.5 mg of cobalt to be dissolved, $E_f = 0.50$ mol F^{-1}. During the electrolysis process, hydrogen was evolved at the cathode. The resulting solid was filtered off, washed with acetonitrile and ether and characterized as $[Co_2L_2]$ H_2O (**1**) (0.032 g, 79%). Elemental analysis: calcd (%) for $C_{48}H_{54}Co_2N_4O_5$:C, 65.2; H, 6.2, N, 6.3; found: C 65.1, H 6.2, N 6.3. IR (KBr, ν, cm^{-1}) 1610(s), 1553(m), 1494(s), 1454(m), 1309(vs), 1210(s), 1102(vs), 1021(m), 962(m), 874(s), 769(m); EI MS m/z; 867 $[Co_2L_2]^+$, 434 $[CoL]^+$, 377 $[H_2L]^+$. Air concentration of the resulting solution yielded a dark violet crystalline solid suitable for X-ray studies.

Synthesis of $[Ni_3L_3]$ (2). An experiment similar to that described above was performed, with nickel as the anode and a solution of H_2L (0.035 g, 0.093 mmol) and tetramethylammonium perchlorate (*ca.* 10 mg) in acetonitrile (80 cm^3), at 5 mA and 6 V for 1 h, dissolved 5.4 mg of nickel (E_f = 0.49). A green solid characterized as $[Ni_3L_3]$ (**2**) was obtained (0.033 g, 82%). Elemental analysis: calcd (%) for $C_{72}H_{78}Ni_3N_6O_6$: C 66.6, H 6.1, N 6.3; found C 66.6, H 6.1, N 6.4. IR (KBr, ν, cm^{-1}): = 1609(s), 1497(vs), 1457(m), 1409(m), 1322(s), 1103(vs), 1053(m), 1021(m), 952(m), 872(m), 761(m); EI MS m/z; 1300 $[Ni_3L_3]^+$; 867 $[Ni_2L_2]^+$; 433 $[NiL]^+$; 377 $[H_2L]^+$;. Crystals suitable for X-ray studies were obtained by crystallization from acetonitrile/dichloromethane.

Synthesis of $[Ni_2L_2(H_2O)_{1.5}]\cdot CH_3CN$ (3). A solution of the ligand (0.035 g, 0.093 mmol) and tetramethylammonium perchlorate (*ca.* 10 mg) in acetonitrile containing 10% in volume of water (80 cm^3) was electrolyzed at 8 V and 5 mA during 1 h; 5.3 mg of nickel metal was dissolved from the anode, $E_f = 0.48$ mol F^{-1}. After the electrolysis the clear solution was filtered to remove any solid impurities and crystals of $[Ni_2L_2(H_2O)_{1.5}]\cdot CH_3CN$ (**3**) suitable for X-ray studies were obtained by air concentration (0.036 g, 84%). Elemental analysis: calcd (%) for $C_{50}H_{58}Ni_2N_5O_{5.5}$: C, 64.3, H, 6.3, N, 7.5; found: C 64.2, H 6.2, N 7.5. IR (KBr, ν, cm^{-1}) 1609(s), 1556(m), 1489(vs), 1455(m), 1410(m), 1323(s), 1107(vs), 1025(m), 971(m). EI MS m/z; 867 $[Ni_2L_2]^+$; 377 $[H_2L]^+$.

Synthesis of $[Cu_2L_2]\cdot 3H_2O$ (4). Electrolysis of a solution of the ligand (0.035 g, 0.093 mmol) and tetramethylammonium perchlorate (*ca.* 10 mg) in acetonitrile (80 cm^3) at 8 V and 5 mA for 1 h dissolved 11.4 mg of copper from the anode, $E_f = 0.96$ mol F^{-1} was performed. The solid obtained in the cell was collected by filtration washed with acetonitrile and ether and characterized as $[Cu_2L_2]\cdot 3H_2O$ (**4**) (0.033 g, 76%). Elemental analysis calcd. (%) for $C_{48}H_{58}Cu_2N_4O_7$: C, 62.0., H, 6.3, N, 6.0; found: C 62.6, H 6.1, N 6.2. IR (KBr, ν, $cm^{-1)}$ 1612(s), 1487(s), 1456(s), 1410(m), 1317(s), 1100(vs), 1029(m), 791(m); EI MS m/z: 876 $[Cu_2L_2]^+$; 437 $[CuL]^+$; 377 $[H_2L]^+$. Slow air evaporation of the solvent from mother liquor provided brown crystals suitable for X-ray studies.

X-ray crystallographic studies

Intensity data for compounds **1–4** were collected using a Smart-CCD-1000 Bruker diffractometer (Mo-Kα radiation, $\lambda = 0.71073$ Å) equipped with a graphite monochromator. Compound **1** was measured at 100 K and data for compounds **2–4** were collected at 120 K. The ω scan technique was employed to measure intensities in all crystals. Decomposition of the crystals did not occur during data collection. The intensities of all data sets were corrected for Lorentz and polarization effects. Absorption effects in all compounds were corrected using the program SADABS.[28] The crystal structures of all compounds were solved by direct methods. Crystallographic programs used for structure solution and refinement were those of SHELX97.[29] Scattering factors were those provided with the SHELX program system. Missing atoms were located in the difference Fourier map and included in subsequent refinement cycles. The structures were refined by full-matrix least-squares refinement on F^2, using anisotropic displacement parameters for all non-hydrogen atoms. Hydrogen atoms not involved in hydrogen bonding were placed geometrically and refined using a riding model with U_{iso} constrained at 1.2 (for non-methyl groups) and 1.5 (for methyl groups) times U_{eq} of the carrier C atom. In the last cycles of refinement of all structures a weighting scheme was used, where weights were calculated using the following formula $w = 1/[\sigma^2(F_o^2) + (aP)^2 + bP]$, where $P = (F_o^2 + 2F_c^2)/3$.

In compound **3**, the refinement of oxygen O(6) as one full oxygen atom gives a U_{iso} value that is too large in comparison to the rest of the atoms in the complex. The large U_{iso} suggests that this position is only partially occupied by an oxygen atom. This oxygen atom O(6) is part of a water molecule coordinated to the nickel atom Ni(2). The Ni–O bond length for this water, 2.324(8) Å, indicates that this water is only weakly bound to the nickel atom and therefore subject to higher vibration. In order to obtain the value for the occupancy parameter for this oxygen, U_{iso} was fixed at a value of 0.045, which is comparable to the value of the terminal methyl groups. The occupancy parameter obtained was 0.4687. This value was then rounded to 0.5 and used in subsequent refinement cycles, giving a U_{iso} of 0.06368. This compound **3** has disordered solvents in the void of the crystal lattice. The contents of this void are half acetonitrile molecule and two half independent water molecules. The solvent molecules in the void have been refined isotropically. Hydrogen atoms for the two lattice water molecules were not modelled. The half acetonitrile molecule is very close to the weakly bound water, O(6), and the chemical meaning is that the weakly bound water is only present in half the complexes, so half of the unit cells have a dimer with two six-coordinated nickel atoms and two water molecules in a void, while the other half of the unit cells have a dimer with one six-coordinated nickel atom and one five-coordinated nickel atom along with an acetonitrile molecule in a void.

The crystal structure of compound **1** presents one molecule of water hydrogen-bonded to the cobalt complex. This molecule could be located and refined. The structure of compound **1** also presents one molecule of acetonitrile per cell in the voids of the crystal lattice which does not interact with the complex and is highly disordered. This molecule was removed using the Squeeze program[30] implemented in Platon.[31] The electron count for the voids in the cell (40 electrons) agrees with the presence of a molecule of acetonitrile (22 electrons) on a general position in the space group *P*-1. Likewise, in the crystal structure of compound **4** three molecules of water, hydrogen-bonded to the copper complex, could be refined. The remaining solvent molecules are located in voids of the lattice and were removed using the Squeeze program. The electron count for the voids (125 electrons) agrees with the presence of one molecule of water (10 electrons) and one molecule of acetonitrile (22 electrons) on a general position in the space group $P2(1)/c$. Finally, the crystal structure of compound **2** also presents highly disordered solvent molecules located in the voids of the crystal lattice. The disorder for these molecules was so severe that they were removed using Squeeze. The total electron count for the voids in the cell (795 electrons) refer to one molecule of acetonitrile (22 electrons) and two molecules of dichloromethane (42 electrons) on a general position in the space group $C2/c$.

Pertinent details of the data collections and structure refinements are summarized in Table 1. Important geometrical data for all compounds are listed in Tables 1–5. Further details regarding the data collections, structure solutions and refinements are included in the ESI.† Ortep3[32] drawings with the numbering schemes used are shown in Figs. 2–5.

Results and discussion

Synthesis of the complexes

The new metal complexes were obtained by electrochemical oxidation of the appropriate cobalt, nickel or copper metal in a cell containing an acetonitrile solution of the ligand. Elemental analysis shows that metal ions react with the ligands in a 1:1 molar ratio to afford complexes of the bis(deprotonated) ligand (L^{2-}). The use of nickel as the anode in a cell containing a solution of the ligand in acetonitrile containing 10% in volume of water allowed the synthesis of $[Ni_2L_2(H_2O)_{1.5}]\cdot CH_3CN$ (**3**).

In the synthesis of nickel and cobalt complexes the electrochemical efficiency values, E_f, were close 0.5 mol F^{-1} (*see experimental part*) and these are consistent with the following reaction scheme:

Cathode: $[H_2L] + 2e^- \rightarrow H_{2(g)} + [L^{2-}]$

Anode: $M \rightarrow M^{2+} + 2\,e^-$

Overall: $[H_2L] + M \rightarrow [ML] + H_2$

M = Co and Ni.

In the synthesis of the copper complex, an E_f value close to 1.0 mol F^{-1} is indicative that the anionic oxidation leads initially to the Cu(I) metal. However, the analytical data show that the final compound is [CuL]. This suggests a subsequent oxidation in solution from Cu(I) to Cu(II) as soon as it is formed, according to the following reaction scheme:

Cathode: $[H_2L] + e^- \rightarrow \frac{1}{2}\,H_{2(g)} + [HL^-]$

Anode: $Cu \rightarrow Cu^+ + e^-$

Solution: $[HL^-] + Cu^+ \rightarrow [CuL] + \frac{1}{2}\,H_{2(g)}$

This behavior has been observed previously in the synthesis of other Cu(II) complexes with related ligands using an electrochemical procedure.[33]

The neutral complexes are sparingly soluble in common organic solvents but they are soluble in polar coordinating solvents such as DMSO and DMF. The compounds appear to be stable in the solid state and in solution. The structural studies (*see below*) show the presence of the dimeric species $[Co_2L_2]\cdot H_2O$ (**1**) and $[Cu_2L_2]\cdot 3H_2O$ (**4**). In the case of nickel, the compound is the

Table 1 Summary of crystallographic data and structure refinement

Compound	**1**	**2**	**3**	**4**
Empirical formula	$C_{48}H_{54}Co_2N_4O_5$	$C_{72}H_{78}N_6Ni_3O_6$	$C_{49}H_{58.50}N_{4.5}Ni_2O_{6.5}$	$C_{48}H_{58}Cu_2N_4O_7$
Formula weight	884.81	1299.53	931.92	930.06
Crystal size, mm	$0.50 \times 0.41 \times 0.23$	$0.38 \times 0.31 \times 0.30$	$0.17 \times 0.17 \times 0.09$	$0.21 \times 0.17 \times 0.09$
Temperature, K	100(2)	120(2)	120(2) K	120(2)
Wavelength	0.71073	0.71073	0.71073	0.71073
Crystal system	Triclinic	Monoclinic	Monoclinic	Monoclinic
Space group	*P*-1	*C* 2/*c*	*P* 2(1)/*n*	*P* 2(1)/*c*
Unit cell dimens.				
a, Å	10.886(4)	51.673(9)	14.083(6)	10.694(2)
b, Å	11.807(4)	13.205(2)	17.120(7)	22.640(4)
c, Å	20.893(7)	21.820(4)	19.394(8)	20.273(4)
α/°	85.537(6)	90	90.	90
β/°	75.688(5)	101.747(3)	104.000(7)	95.394(3)
γ/°	63.367(5)	90	90	90
Volume, Å^3	2324.3(14)	14577(4)	4537(3)	4886.9(16)
Z	2	8	4	4
μ, mm^{-1}	0.761	0.818	0.885	0.921
No. reflections collectec.	29164	62460	38942	77473
No. of independent reflections	10551 [*R*(int) = 0.0296]	14836 [*R*(int) = 0.0418]	9334 [*R*(int) = 0.1172]	10130 [*R*(int) = 0.1015]
Data/restraints/parameters	10551/1/546	14836/0/797	9334/4/582	10130/6/576
Goodness-of-fit	1.066	1.093	0.932	1.078
Final *R* indices [$I > 2\sigma(I)$]	$R1^a = 0.0318$	$R1 = 0.0346$	$R1 = 0.0597$	$R1 = 0.0502$
	$wR2^b = 0.0799$	$wR2 = 0.0875$	$wR2 = 0.1266$	$wR2 = 0.1187$

^{a} $R1 = \sum[|F_o| - |F_c|/\sum|F_o|]$; ^{b} $wR2 = [|\sum(F_o^2 - F_c^2)/\sum(F_o^2)]^{1/2}$.

trimeric species $[Ni_3L_3]$ (**2**), although when the synthesis was carried out in acetonitrile/water solution the species obtained was the dimer $[Ni_2L_2(H_2O)_{1.5}]\cdot CH_3CN$ (**3**).

Description of structures. Compounds **1–4** were studied by X-ray diffraction.†

Structure of $[Co_2L_2]\cdot H_2O$ (1). The molecular structure of **1** is shown in Fig. 1 together with the atom labeling scheme adopted. A selection of bond distances and angles, with the estimated standard deviations, is given in Table 2.

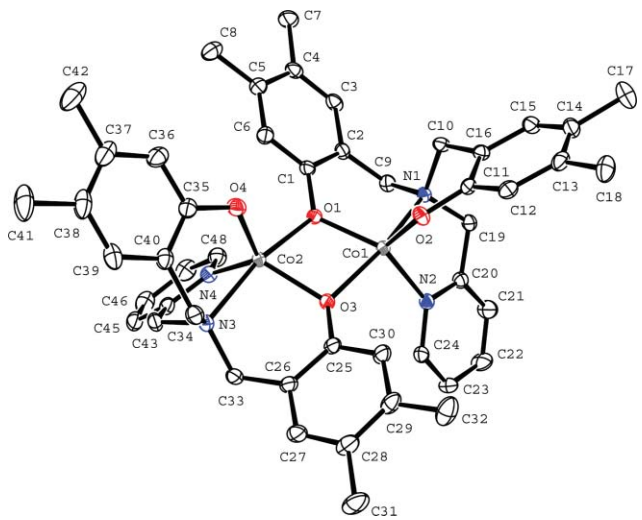

Fig. 1 ORTEP diagram of the molecular structure of **1** with 50% thermal ellipsoid probability.

The molecular structure of **1** consists of a dinuclear species with the cobalt atom pentacoordinated by two nitrogen atoms and two phenoxo oxygen atoms of a bis(deprotonated) Mannich base ligand and also by another bridging phenoxo oxygen atom from another similar fragment.

Analysis of the shape-determining bond angles, using the geometrical parameter τ [$\tau = (\beta - \alpha)/60$][34] gives values of 0.65 and 0.71 for the two cobalt atoms and suggests that they are in an environment close to a $[CoN_2O_3]$ trigonal bipyramid ($\tau = 1$) with the two phenoxo oxygen atoms and the pyridine nitrogen atom of a tetradentate ligand in the equatorial plane and the other nitrogen atom of the same ligand and the bridging oxygen atom from the other ligand in the apical positions. The two coordination polyhedra are joined through the edge that contains the two bridging oxygen atoms.

The four-membered ring formed by the two cobalt atoms and the two oxygen atoms, *i.e.* Co(1)–O(1)–O(3)–Co(2), is nearly planar (r.m.s. deviation of 0.0882). However, the bridge is slightly asymmetric, with two shorter bond distances [Co(1)–O(1) 1.9744(12) and Co(2)–O(3) 1.9965(12) Å] and two longer distances [Co(1)–O(3) 2.0820(12) and Co(2)–O(1) 2.0427(12) Å]. These bond distances are slightly longer than those corresponding to the metal and oxygen phenoxo terminal atoms, Co(1)–O(2) 1.9341(12) and Co(2)–O(4) 1.9222(12) Å, respectively. However, all bond distances are in the range of average values for Co–O(phenoxo) bonds observed in other pentacoordinated Co(II) complexes.[35–38] The two cobalt(II) centers are separated by 3.1192(8) Å, a value that is similar to those found in other phenoxo-bridged dinuclear cobalt compounds.[35,36]

The two Co–N(amine) distances are similar, Co(1)–N(1) 2.1982(14) Å and Co(2)–N(3) 2.1699(14) Å, and are close to the same bond distances in other pentacoordinated cobalt complexes, *i.e.* in the range 2.092(4)–2.197(5) Å.[35–38,39] The Co–N(pyridine) bonds, 2.0865(14) and 2.0710(15) Å, are slightly shorter but are also in the normal range observed in pentacoordinated cobalt(II) complexes of pyridine derivatives [2.068–2.174 Å].[40]

Table 2 Selected bond lengths (Å) and angles (deg) for $[Co_2L_2]\cdot H_2O$ (**1**)

Co(1)–O(2)	1.9341(12)	Co(2)–O(4)	1.9222(12)
Co(1)–O(1)	1.9744(12)	Co(2)–O(3)	1.9965(12)
Co(1)–O(3)	2.0820(12)	Co(2)–O(1)	2.0427(12)
Co(1)–N(2)	2.0865(14)	Co(2)–N(4)	2.0710(15)
Co(1)–N(1)	2.1982(14)	Co(2)–N(3)	2.1699(14)
Co(1)–Co(2)	3.1192(8)		
O(2)–Co(1)–O(1)	117.83(5)	O(4)–Co(2)–O(3)	116.10(5)
O(2)–Co(1)–O(3)	103.79(5)	O(4)–Co(2)–O(1)	101.70(5)
O(1)–Co(1)–O(3)	78.10(5)	O(3)–Co(2)–O(1)	78.54(4)
O(2)–Co(1)–N(2)	115.89(5)	O(4)–Co(2)–N(4)	119.18(6)
O(1)–Co(1)–N(2)	125.17(5)	O(3)–Co(2)–N(4)	124.21(5)
O(3)–Co(1)–N(2)	99.28(5)	O(1)–Co(2)–N(4)	96.99(6)
O(2)–Co(1)–N(1)	91.02(5)	O(4)–Co(2)–N(3)	91.02(5)
O(1)–Co(1)–N(1)	89.75(5)	O(3)–Co(2)–N(3)	92.78(5)
O(3)–Co(1)–N(1)	164.01(5)	O(1)–Co(2)–N(3)	166.80(5)
N(2)–Co(1)–N(1)	79.14(5)	N(4)–Co(2)–N(3)	79.57(6)
Co(1)–O(1)–Co(2)	101.86(5)	Co(1)–O(3)–Co(2)	99.75(5)

The bond lengths and angles for the ligand are as expected, with values close to those found in other complexes with related ligands. In all cases, the C–O bond lengths have intermediate values between a typical C–O single bond and a C=O double bond.[41]

This compound crystallizes with one non-coordinated water molecule. This molecule is hydrogen bonded to the two phenoxo oxygen atoms not involved in the Co_2O_2 bridge, O(2) and O(4).

Structure of $[Ni_3L_3]$ (2). The molecular structure of **2** is shown in Fig. 2 along with the atom labeling scheme adopted. A selection of bond lengths and angles with the estimated standard deviations are given in Table 3.

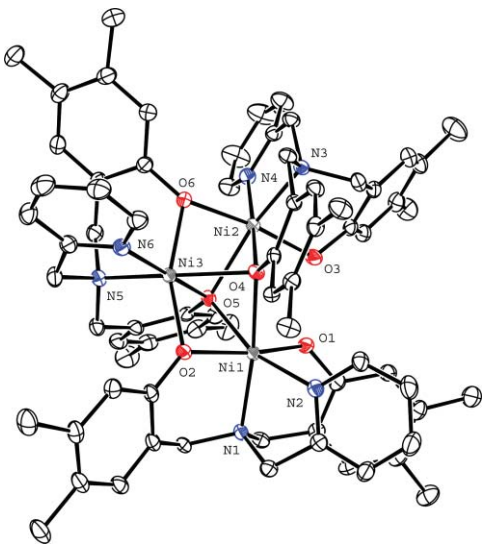

Fig. 2 ORTEP diagram of the molecular structure of **2** with 50% thermal ellipsoid probability.

The structure consists of trimeric species in which three nickel atoms are coordinated to three bis(deprotonated) Mannich bases with four phenoxo oxygen atoms bridging the nickel atoms. The ligands are all tetradentate but show different coordination behavior. A first ligand acts as an N(1)N(2) chelate, an oxygen atom O(1) acts as terminal and O(2) acts as a bridge between two nickel atoms. A second ligand also acts as an N(3)N(4) chelate, the O(3) acts as terminal and a third oxygen atom O(4) as triple oxo-bridge. Finally, the third ligand is bonded to the metals through both amine N(5) and pyridine N(6) nitrogen atoms, a phenoxo oxygen atom O(5) acts as a triple bridge between the three metal atoms and, finally, the other oxygen atom O(6) bridges two metal atoms.

The three nickel atoms are in a distorted octahedral $[N_2O_4]$ environment and, on the whole, the structure can be considered as consisting of a central Ni(3) octahedron sharing two contiguous triangular faces, with O(2)O(4)O(5) belonging to the Ni(1) octahedron and O(4)O(5)O(6) to the Ni(2) octahedron. Thus, the Ni(1), Ni(2) and Ni(3) octahedra share a common edge, O(4)–O(5) (Fig. 3).

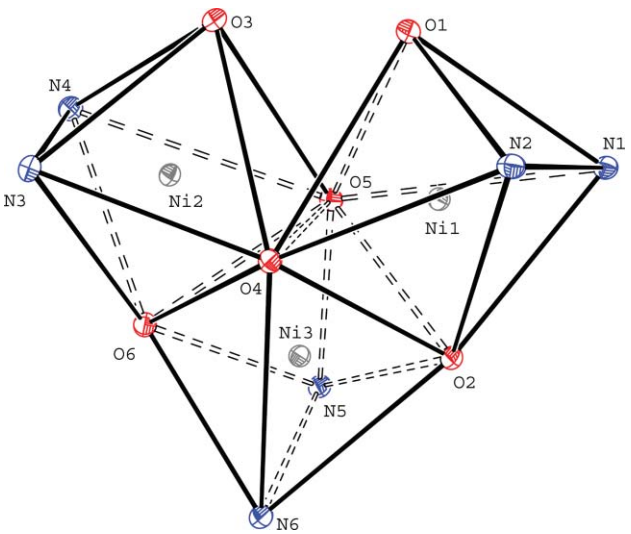

Fig. 3 A partial view of the coordination sphere of the metals in **2**.

The bond distances between the nickel atoms and the phenoxo oxygens are in the range 2.0053(14)–2.2386(14) Å and these are significantly different to one another, with the longest distances corresponding to the oxygen atoms O(5) and O(4), which establish triple bridges between the metal centers. The shortest distances are very similar to those observed in other dinuclear and trinuclear Ni(II) derivatives containing oxygen bridging atoms.[42–46]

Table 3 Selected bond distances (Å) and angles (deg) for $[Ni_3L_3]$ (**2**)

Ni(1)–O(2)	2.0103(14)	Ni(1)–O(5)	2.1956(14)
Ni(1)–O(1)	2.0313(14)	Ni(2)–O(3)	2.0195(14)
Ni(1)–O(4)	2.1801(13)	Ni(2)–O(6)	2.0452(14)
Ni(1)–N(2)	2.0598(17)	Ni(2)–N(4)	2.0480(17)
Ni(1)–N(1)	2.1245(16)	Ni(2)–N(3)	2.0676(17)
Ni(2)–O(4)	2.0734(13)	Ni(2)–O(5)	2.2386(14)
Ni(3)–O(6)	2.0053(14)	Ni(3)–O(2)	2.0241(14)
Ni(3)–N(6)	2.0555(17)	Ni(3)–O(5)	2.0582(13)
Ni(3)–N(5)	2.0612(17)	Ni(3)–O(4)	2.1939(14)
Ni(1)–Ni(3)	2.9047(5)	Ni(2)–Ni(3)	2.8195(5)
O(2)–Ni(1)–O(1)	163.18(6)	O(3)–Ni(2)–O(6)	172.50(6)
O(2)–Ni(1)–N(2)	112.05(6)	O(3)–Ni(2)–N(4)	87.92(6)
O(1)–Ni(1)–N(2)	84.71(6)	O(6)–Ni(2)–N(4)	93.79(6)
O(2)–Ni(1)–N(1)	91.74(6)	O(3)–Ni(2)–N(3)	90.54(6)
O(1)–Ni(1)–N(1)	89.58(6)	O(6)–Ni(2)–N(3)	96.90(6)
N(2)–Ni(1)–N(1)	80.75(6)	N(4)–Ni(2)–N(3)	83.97(7)
O(2)–Ni(1)–O(4)	79.38(5)	O(5)–Ni(2)–O(4)	69.74(5)
O(1)–Ni(1)–O(4)	99.71(5)	O(3)–Ni(2)–O(4)	96.64(6)
N(2)–Ni(1)–O(4)	99.93(6)	O(6)–Ni(2)–O(4)	82.03(5)
N(1)–Ni(1)–O(4)	170.71(6)	O(4)–Ni(2)–N(4)	174.71(6)
O(1)–Ni(1)–O(5)	83.27(5)	O(4)–Ni(2)–N(3)	93.26(5)
N(2)–Ni(1)–O(5)	161.70(6)	O(3)–Ni(2)–O(5)	89.25(5)
N(1)–Ni(1)–O(5)	112.86(6)	O(6)–Ni(2)–O(5)	83.36(5)
O(4)–Ni(1)–O(5)	68.70(5)	N(4)–Ni(2)–O(5)	113.15(6)
O(2)–Ni(1)–O(5)	80.77(5)	N(3)–Ni(2)–O(5)	162.85(6)
O(6)–Ni(3)–O(2)	158.75(6)	O(6)–Ni(3)–N(6)	88.34(6)
O(2)–Ni(3)–N(6)	100.23(6)	O(6)–Ni(3)–O(5)	89.15(5)
O(2)–Ni(3)–O(5)	83.89(5)	N(6)–Ni(3)–O(5)	174.25(6)
O(6)–Ni(3)–N(5)	94.22(6)	O(2)–Ni(3)–N(5)	105.90(6)
N(6)–Ni(3)–N(5)	84.11(7)	O(5)–Ni(3)–N(5)	90.91(6)
O(6)–Ni(3)–O(4)	80.00(5)	O(2)–Ni(3)–O(4)	78.76(5)
N(6)–Ni(3)–O(4)	113.70(6)	O(5)–Ni(3)–O(4)	70.91(5)
N(5)–Ni(3)–O(4)	160.86(6)	Ni(1)–O(5)–Ni(2)	99.50(5)
Ni(2)–O(4)–Ni(1)	105.41(5)	Ni(1)–O(4)–Ni(3)	83.22(5)
Ni(1)–O(2)–Ni(3)	92.10(6)	Ni(2)–O(4)–Ni(3)	82.66(5)
Ni(3)–O(5)–Ni(1)	86.07(5)	Ni(2)–O(6)–Ni(3)	88.22(5)
Ni(3)–O(5)–Ni(2)	81.90(5)		

The Ni–N(amine) bond distances, although slightly different to one another [Ni(1)–N(1) 2.1245(16) Å, Ni(2)–N(3) 2.0676(17) Å and Ni(3)–N(5) 2.0612(17) Å], are analogous to those found in hexacoordinated trinuclear Ni(II) complexes,[46–49] *e.g.* in $[Ni_3L'_2(OAc)_2(NCS)_2]$ (L' = 2-butyliminomethyl-4-methyl-6{[methyl-(2-pyridin-2-ethyl)amino]methyl}phenol)[50] or in the dimeric species **3** described in this work. The Ni–N(pyridine) bond distances, 2.0480(17)–2.0598(17) Å, are the same as those found in other hexacoordinated Ni(II) complexes with ligands derived from pyridine.[51–54]

In the dianionic Mannich ligand the bond distances and angles are as expected and are similar to the distances and angles found in other complexes that contain this ligand.

Structure of $[Ni_2L_2(H_2O)_{1.5}]\cdot CH_3CN$ (3). In compound **3** the water molecule O(5) located above Ni(1) is a whole and normal water molecule. However, within the network only half of the cells contain Ni(2) weakly coordinated by a second water molecule O(6) and, as such, this can be considered as half a water molecule. The molecular structure of the complex that contains the two water molecules is shown in Fig. 4 along with the atom labeling scheme adopted. A selection of bond lengths and angles with the estimated standard deviations are given in Table 4.

The structure consists of binuclear species in which each metal atom is coordinated to two nitrogen and two oxygen atoms from a tetradentate bi-deprotoned Mannich base ligand. The coordination is completed by an oxygen atom from another similar fragment, which acts as a bridge between metal atoms. In the environment of Ni(1) there is an oxygen atom from a water molecule that, with a bond distance of 2.096(3) Å, establishes a normal covalent bond with the metal atom. Within the network half of the cells contain a second water molecule, the oxygen atom of which is coordinated to the Ni(2) atom with a bond distance of 2.328(7) Å. This indicates a weaker interaction in this case. As such, it can be considered that Ni(1) is always hexacoordinated while Ni(2) is hexacoordinated in only half of the cases and pentacoordinated in the other half.

Each bridging phenoxo oxygen atom is more or less symmetrically bound, with Ni–O bond distances in the range between 2.080(3) [Ni(1)–O(4)] and 2.034(3) Å [Ni(2)–O(4)]. These distances are fairly similar to those found between the nickel and the terminal phenoxo oxygen atoms [Ni(1)–O(1) = 2.017(3), Ni(2)–O(3) = 1.968(3) Å]. Neither of these distances falls outside the range of average Ni–O(phenoxo) distances observed in other hexacoordinated nickel(II) complexes [1.971(2)–2.102(7) Å].[42–46] The nickel atoms are separated by 3.2076(13) Å, a distance that is close to those found in other similar dinuclear nickel compounds.[47–49]

The Ni(1)–O(5) bond distance [2.096(3) Å] is as expected and is similar to those described above. However, the Ni(2)–O(6) bond distance [2.328(7) Å] is considerably longer and this is

Table 4 Selected bond lengths (Å) and angles (deg) for $[Ni_2L_2(H_2O)_{1.5}]\cdot CH_3CN$ (**3**)

Ni(1)–O(1)	2.017(3)	Ni(1)–O(2)	2.060(3)
Ni(1)–O(4)	2.080(3)	Ni(1)–O(5)	2.096(3)
Ni(1)–N(2)	2.096(4)	Ni(2)–O(3)	1.968(3)
Ni(1)–N(1)	2.126(4)	Ni(2)–O(4)	2.034(3)
Ni(2)–O(2)	2.035(3)	Ni(2)–N(4)	2.039(4)
Ni(2)–N(3)	2.126(4)	Ni(2)–O(6)	2.328(7)
Ni(1)–Ni(2)	3.2076(13)		
O(1)–Ni(1)–O(2)	172.72(11)	O(1)–Ni(1)–O(4)	98.40(11)
O(2)–Ni(1)–O(4)	76.32(11)	O(1)–Ni(1)–O(5)	87.32(12)
O(2)–Ni(1)–O(5)	87.37(12)	O(4)–Ni(5)–O(5)	86.75(12)
O(1)–Ni(1)–N(2)	91.47(12)	O(2)–Ni(1)–N(2)	94.42(12)
O(4)–Ni(1)–N(2)	100.46(13)	O(5)–Ni(1)–N(2)	172.79(14)
O(1)–Ni(1)–N(1)	93.10(12)	O(2)–Ni(1)–N(1)	92.10(12)
O(4)–Ni(1)–N(1)	168.41(12)	O(5)–Ni(1)–N(1)	92.36(13)
N(2)–Ni(1)–N(1)	80.61(14)	O(3)–Ni(2)–O(4)	159.65(13)
O(3)–Ni(2)–O(2)	94.15(12)	O(4)–Ni(2)–O(2)	77.91(11)
O(3)–Ni(2)–N(4)	107.83(14)	O(4)–Ni(2)–N(4)	92.32(13)
O(2)–Ni(2)–N(4)	103.71(13)	O(3)–Ni(2)–N(3)	91.97(13)
O(4)–Ni(2)–N(3)	93.90(12)	O(2)–Ni(2)–N(3)	170.45(12)
N(4)–Ni(2)–N(3)	81.31(14)	O(3)–Ni(2)–O(6)	69.3(2)
O(4)–Ni(2)–O(6)	90.9(2)	O(2)–Ni(2)–O(6)	82.5(2)
N(4)–Ni(2)–O(6)	173.5(2)	N(3)–Ni(2)–O(6)	92.9(2)
Ni(1)–O(2)–Ni(2)	103.09(13)	Ni(1)–O(4)–Ni(2)	102.46(12)

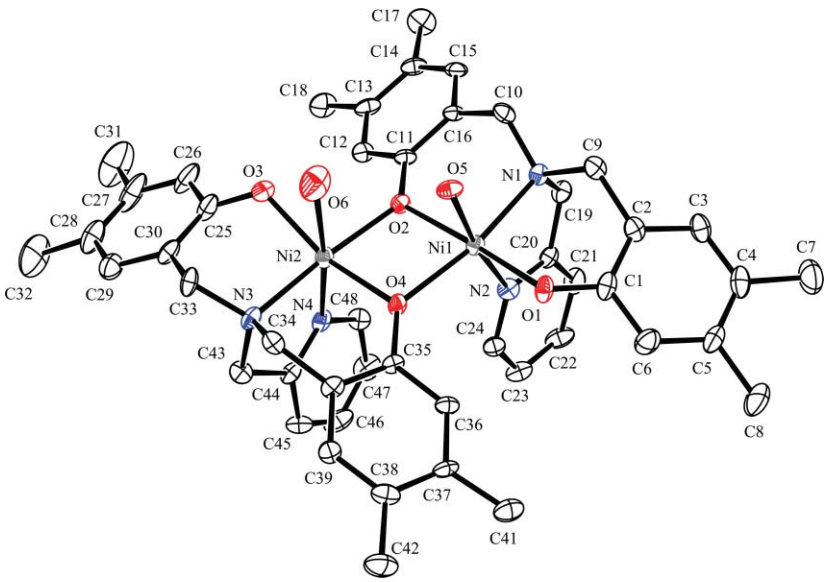

Fig. 4 ORTEP diagram of the molecular structure of **3** with 50% thermal ellipsoid probability.

indicative of a weak interaction between the two atoms. Finally, the Ni–N(amine) bond distances and Ni–N(pyridine) bond distances are normal and similar to those found in the trimer complex described above. As such these data do not warrant any further comment.

The compound contains an acetonitrile molecule of crystallization that does not interact with the cobalt complex in any significant manner.

Crystal Structure of $[Cu_2L_2]\cdot 3H_2O$ (4). A view of compound **4** is shown in Fig. 5 together with the atomic labeling scheme used. A selection of bond distances and angles (with the estimated standard deviations) are given in Table 5.

The structure of the complex consists of $[Cu_2L_2]$ dimers in which each metal atom is pentacoordinated by an amine nitrogen, a pyridine nitrogen and two oxygen atoms of a bis(deprotonated) ligand. The coordination is completed by a bridging oxygen atom from another similar fragment. The Cu_2O_2 bridge is essentially planar (r.m.s. 0.0843). The bridge is clearly asymmetric, with two longer bond distances [Cu(1)–O(2) 2.149(2), Cu(2)–O(4) 2.144(2) Å] and two shorter distances [Cu(1)–O(4) 1.930(2), Cu(2)–O(2) 1.950(2) Å]. The two metal centers are separated by 3.1342 Å.

The values of 0.30 for Cu(1) and 0.25 for Cu(2) found for the trigonality index τ suggest that the metal atoms are in an environment close to square pyramidal,[34] with bridging oxygen atoms occupying apical positions and the oxygen atoms not involved in the bridge in a *syn* disposition with respect to the Cu_2O_2 core. Both square pyramids share the common basal edge defined by the bridging O2 and O4 and their bases are inverted.

Table 5 Selected bond distances (Å) and angles (deg) for $[Cu_2L_2].3H_2O$ (**4**)

Cu(1)–O(4)	1.930(2)	Cu(2)–O(2)	1.950(2)
Cu(1)–O(1)	1.939(2)	Cu(2)–O(3)	1.958(2)
Cu(1)–N(2)	2.009(3)	Cu(2)–N(4)	2.015(3)
Cu(1)–N(1)	2.027(3)	Cu(2)–N(3)	2.046(3)
Cu(1)–O(2)	2.149(2)	Cu(2)–O(4)	2.144(2)
O(4)–Cu(1)–O(1)	96.61(10)	O(2)–Cu(2)–O(3)	98.04(10)
O(4)–Cu(1)–N(2)	89.69(11)	O(2)–Cu(2)–N(4)	91.30(11)
O(1)–Cu(1)–N(2)	150.66(11)	O(3)–Cu(2)–N(4)	151.38(10)
O(4)–Cu(1)–N(1)	168.66(10)	O(2)–Cu(2)–N(3)	166.43(10)
O(1)–Cu(1)–N(1)	94.39(10)	O(3)–Cu(2)–N(3)	93.65(11)
N(2)–Cu(1)–N(1)	82.00(11)	N(4)–Cu(2)–N(3)	81.56(12)
O(4)–Cu(1)–O(2)	79.29(9)	O(2)–Cu(2)–O(4)	79.00(9)
O(1)–Cu(1)–O(2)	104.11(9)	O(3)–Cu(2)–O(4)	103.00(9)
N(2)–Cu(1)–O(2)	105.21(10)	N(4)–Cu(2)–O(4)	105.33(10)
N(1)–Cu(1)–O(2)	95.40(10)	N(3)–Cu(2)–O(4)	91.72(10)
Cu(2)–O(2)–Cu(1)	99.66(9)	Cu(1)–O(4)–Cu(2)	100.48(9)

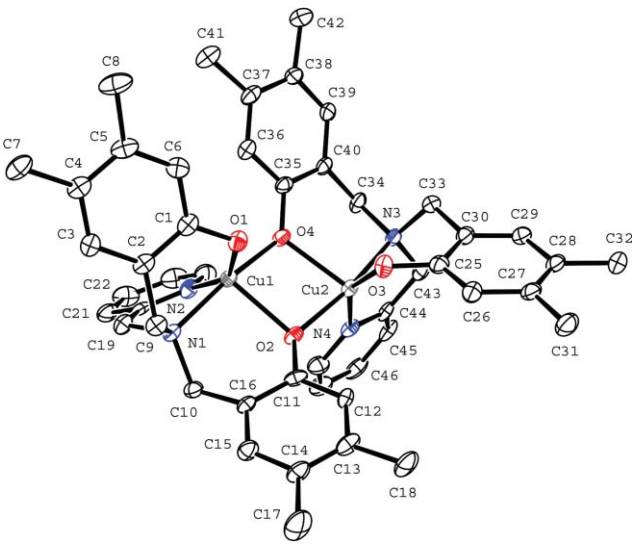

Fig. 5 ORTEP diagram of the molecular structure of **4** with 50% thermal ellipsoid probability.

The bond lengths between the copper and oxygen atoms, although different as a consequence of the asymmetry of the bridge, can be considered as normal and are similar to those found in other pentacoodinated copper(II) complexes containing a bridging phenoxo oxygen.[55] The Cu–N(amine), 2.027(3) and 2.046(3) Å, and Cu–N(pyridine), 2.009(3) and 2.015(3) Å, bond lengths, respectively, are similar and are within the normal range observed in other pentacoordinated copper(II) complexes of amine[55] and/or pyridine[33] ligands.

This compound crystallizes with three non-coordinated water molecules. One of these molecules, O(1 s), is hydrogen-bonded to the two phenoxo oxygen atoms not involved in the Cu_2O_2 bridge, O(1) and O(3). A second molecule, O(2 s) is hydrogen-bonded to one of the phenoxo oxygen atoms not involved in the Cu_2O_2 bridge, O(3). Finally, the third molecule, O(3 s) is hydrogen-bonded to the water molecule O(2 s).

IR spectroscopy and mass spectrometry. In the IR spectra of complexes, the ν(O–H) (at 3350–3100 cm^{-1}) and δ(OH) (at 1241 cm^{-1}) vibrations corresponding to the free ligand are not observed. This fact, along with the presence of a band at 1309–1323 cm^{-1} attributable to ν(CO) (at 1294 cm^{-1} in the free ligand), indicates that phenolic hydrogen atoms are lost during the electrochemical synthesis and that the bis(deprotonated) ligand is coordinated to the metal ions through both phenoxo oxygen atoms.

The electrospray mass spectra of the compounds show the peaks associated with dimer $[M_2L_2]^+$ (*m/z* 867, 867 and 876, respectively, for **1**, **3** and **4** or the trimer $[Ni_3L_3]^+$ (*m/z* 1306), with the appropriate isotope distribution. The spectra also show peaks associated with the loss of one ML unit from the initial species (*m/z* 434, 870 and 437, respectively, for **1**, **2** and **4** and the loss of a second NiL unit in the case of the trimeric nickel complex (*m/z* 433). In all cases the peak due to the free ligand at *m/z* 377 is also observed.

Magnetic properties. The magnetic behavior of **1**, expressed in the form of $\chi_M T$ and χ_M *versus* T, where χ_M is the molar magnetic susceptibility and T the temperature, is depicted in Fig. 6. $\chi_M T$ at 300 K is equal to 4.68 cm^3 K mol^{-1} ($\chi_M = 1.58 \times 10^{-2}$ cm^3 K mol^{-1}) and this value is consistent with two Co(II) ions in the high-spin state ($S = 3/2$, $g = 2.23$). $\chi_M T$ decreases as T decreases, first smoothly down to 75 K and then more rapidly to reach a value of

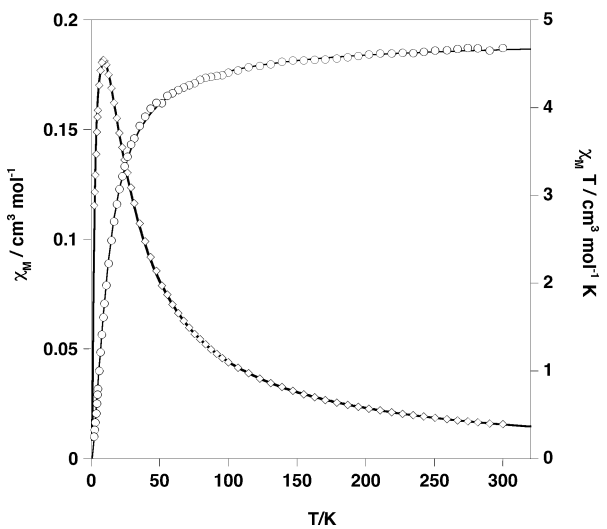

Fig. 6 Magnetic behavior of **1**.

0.25 cm^3 K mol^{-1} at 2 K. χ_M increases continuously from 1.58×10^{-2} at 300 K to reach a maximum, 0.182 cm^3 mol^{-1}, at *ca.* 10 K. Below this temperature χ_M decreases rapidly. This behavior, reminiscent of an intramolecular antiferromagnetic interaction between two Co(II) ions, has been analyzed using an expression of χ_M based on the isotropic Hamiltonian $H = -JS_AS_B$ with $S_A = S_B = 3/2$.[56] The best fit for calculated and experimental data (solid line in Fig. 6) was achieved for $J = -4.2$ cm^{-1}, $g = 2.26$ with $R = 8 \times 10^{-4}$. R corresponds to the agreement factor, which is defined as $\Sigma_i[(\chi_M)_i^{exptl} - [(\chi_M)_i^{calc}]^2/[(\chi_M)_i^{exptl}]^2)$.

The $\chi_M T$ *vs.* T plot for **2** is shown in Fig. 7. At 297 K, the $\chi_M T$ value of 3.39 cm^3 K mol^{-1} is consistent for three Ni(II) ions with $S = 1$ ($g = 2.13$), in agreement with the structural data, which confirm the presence of $[Ni^{II}]_3$ trinuclear species. $\chi_M T$ decreases smoothly down to 50 K, then decreases more rapidly to reach a value of 0.86 cm^3 K mol^{-1} at 2 K, denoting the occurrence of an antiferromagnetic interaction.

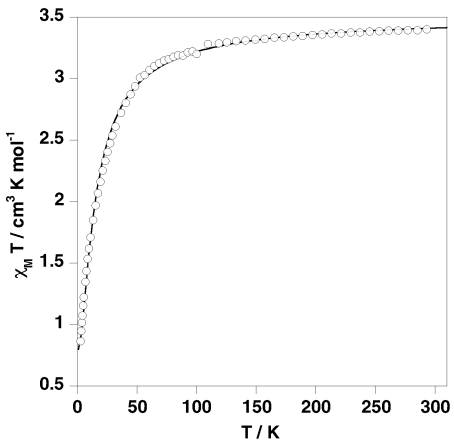

Fig. 7 Magnetic behavior of **2**.

This magnetic behavior was analyzed using a spin Hamiltonian $H = -J(S_{A1}S_B + S_{A2}S_B) - J'(S_{A1}S_{A2})$ characterized by coupling constants J and J', which correspond to two identical pathways Ni(A)–Ni(B) and Ni(A)–Ni(A, respectively (see Scheme 3).[56]

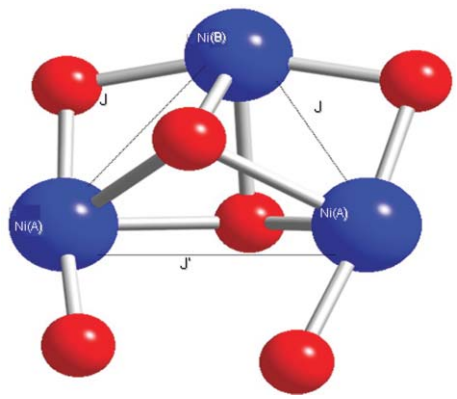

Scheme 3 View of the Ni_3 core of compound **2** indicating the magnetic coupling pathway.

The best fit for calculated and experimental $\chi_M T$ data was achieved for $J = -5.3$ cm^{-1}, $J' = -2.7$ cm^{-1}, $g = 2.16$, $\theta = -0.05$ cm^{-1} and $R = 3 \times 10^{-4}$. The parameter θ was introduced in the expression of the magnetic susceptibility to improve the quality of the fit, usually, it is associated to the intermolecular interactions but here implicitly reflects the occurrence of zero-field splitting of the Ni(II) $S = 1$ ground state.

The $\chi_M T$ *vs.* T plot for **3** is shown in Fig. 8. $\chi_M T$ is equal to 2.05 cm^3 K mol^{-1} at 297 K, a value close to that expected for the contribution of two $S = 1$ spin centers without orbital contribution ($g = 2$). On cooling, $\chi_M T$ decreases continuously almost to zero at 2 K while χ_M increases from 6.9×10^{-3} cm^3 mol^{-1} at 297 K to reach a maximum value of 2.13×10^{-2} cm^3 mol^{-1} at 39 K. Below 39 K, χ_M decreases again to reach a minimum at *ca.* 9 K, from which a new increase is observed.

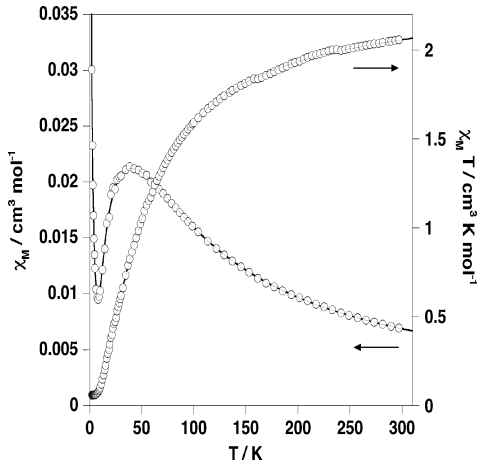

Fig. 8 Magnetic behavior of **3**.

The behavior described above is consistent with the occurrence of antiferromagnetic coupling between the two $S = 1$ centers and the existence of a small paramagnetic impurity. In this case, the occurrence of zero-field splitting in the $S = 1$ local spin state was explicitly taken into account as reported by Ginsberg *et al.*[57] The best fit for calculated and experimental data was achieved for $J = -30$ cm^{-1}, $D = 4.7$ cm^{-1} (the zero-field splitting parameter), $g = 2.14$, ρ (paramagnetic impurities) = 0.05 and $R = 2 \times 10^{-3}$. The calculated values are represented as a solid line in Fig. 8.

The $\chi_M T$ *vs.* T plot for **4** is shown in Fig. 9. At 300 K, $\chi_M T$ has a value close to 0.83 cm^3 K mol^{-1}, which is in the range expected for two Cu(II) ions ($g = 2.10$). In the temperature

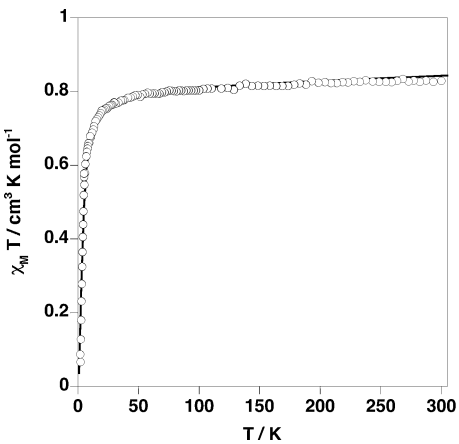

Fig. 9 Magnetic behavior of **4**.

range 300–50 K, $\chi_M T$ remains almost constant while below 50 K it decreases rapidly down to 0.06 cm^3 K mol^{-1}, suggesting the occurrence of very weak antiferromagnetic interactions. These magnetic data were analyzed using the isotropic Heisenberg interaction with $S_A = S_B = \frac{1}{2}$ described for **1**. The resulting χ_M *versus* T expression, the so-called Bleaney–Bowers expression, was implemented to take into account the paramagnetic impurities ρ. The parameters determined by least-squares fit minimizing J, g, and ρ are -4.7 cm^{-1}, $g = 2.12$, $\rho = 0.08$ and $R = 8 \times 10^{-4}$. Temperature-independent paramagnetism (TIP) was considered equal to 120×10^{-6} cm^3 mol^{-1}.

The antiferromagnetic behavior observed for **1**, **3** and **4** is consistent with their structural characteristics. These compounds have quite similar structures, however, they display remarkably different J values. It is well-known that direct comparison between the magnetic coupling values of **1**, **3** and **4** cannot be made because Co(II), Ni(II) and Cu(II) ions differ in the number, n, of unpaired electrons. Consequently, the expected J values can be related as follows: J[Cu(II)] $\approx n^2 J$[Ni(II) or Co(II)].[56] Taking into account that the experimental J value is -30 cm^{-1} for **3**, the expected values for **1** and **4** would be -13 and -120 cm^{-1}, respectively, if the molecular geometries of **1** and **4** were exactly the same as for **3**. The large differences between these values and those found experimentally, -4.2 cm^{-1} (**1**) and -4.7 cm^{-1} (**4**), can be ascribed to structural factors. The coordination geometry of Ni(II) in **3** clearly facilitates a larger overlap between the magnetic orbitals through the bridges, which also define favorable angles Ni(1)–O(2)–Ni(2) = 103.09(13)° and Ni(1)–O(4)–Ni(2) = 102.46(12)° for strong antiferromagnetic interaction. The geometry around Co(II) in **1** is much more distorted and hence less appropriate for magnetic exchange. In addition, the slightly smaller angles Co(1)–O(1)–Co(2) = 101.86(5)° and Co(1)–O(3)–Co(2) = 99.75(5)° with respect to **3**, justify a smaller overlap of the magnetic orbitals at the bridge. In the case of **4** the reason for the small experimental J value is essentially misorientation of the orbitals, $d_{x^2-y^2}$, containing the unpaired electrons. Indeed, the coordination geometry of **4** favors overlapping between the $d_{x^2-y^2}$ and d_{z^2}, and consistently with the structure it is expected for the d_{z^2} orbital to bear very small spin density.

Concerning the trinuclear complex **2**, the antiferromagnetic interaction observed between the triple-bridged peripheral and the central Ni(II) ions [Ni(1)–Ni(3) and Ni(2)–Ni(3)] ($J = -5.3$ cm^{-1}) could be considered an unexpected result at first glance. The angles Ni(1)–O–Ni(3) and Ni(2)–O–Ni(3), found in the interval 82–92° (Table 3), are in the range observed for related relevant examples in which weak-medium ferromagnetic interaction occurs.[58] However, unlike **2**, all the ferromagnetically coupled compounds referred above are constituted of linear trinuclear Ni(II) species (except 58 d). This fact together with the strongly distorted Ni coordination sites may be the cause of the sign of J found in **2**. As far as we know, only one phenoxo-bridged trinuclear Ni(II) complex exhibiting antiferromagnetic interaction has been reported up to now. In this linear trinuclear Ni(II) compound the larger Ni–O–Ni angles, found in the 99.7–100.5° range, account for the observed antiferromagnetic coupling between adjacent Ni(II) ions ($J \approx -16$ cm^{-1}).[59] These angles are close to those observed for the doubly linked Ni(1) and Ni(2) ions in **2**. The smaller magnitude of the coupling constant ($J' = -2.7$ cm^{-1}) found in the latter could be ascribed to the strongly bended Ni(1)O(4)O(5)Ni(2) moiety, which is determined by the dihedral angle defined by the intersection of two connected Ni(II) octahedral basal planes (around 140°). Departure of this angle from 180° reduces drastically the overlap between the orbitals containing the unpaired electrons. This structural parameter could account for the magnitude and even the sign of the coupling constant J involving the Ni(1)–Ni(3) and Ni(2)–Ni(3) pairs. A more definitive correlation between J and the structure of **2** would be expected, however, the available number of magneto-structurally characterized phenoxo-bridged trinuclear Ni(II) complexes is still small.

Catalase-like activity. The catalytic decomposition of H_2O_2 was studied as a model reaction for the catalase. These studies on disproportionation of the H_2O_2 into H_2O and O_2 by the synthesized compounds were carried out under physiological conditions (see experimental part) by the Amplex® Red-HRP method.[23,24]

The synthesized compounds themselves were unable to directly react with the Amplex® Red reagent, which indicates that these compounds do not interfere with the measurements. All of the tested complexes **1–4** (1–25 μM) exhibited a significant catalase-like activity in a concentration-dependent manner (Fig. 10). Analysis of the data was carried out based on the Michaelis–Menten model, which was originally developed for enzyme kinetics. From the Lineweaver–Burk plots a number of parameters were calculated and are listed in Table 5. Similar results have been reported previously for a number of different inorganic complexes.[60–63]

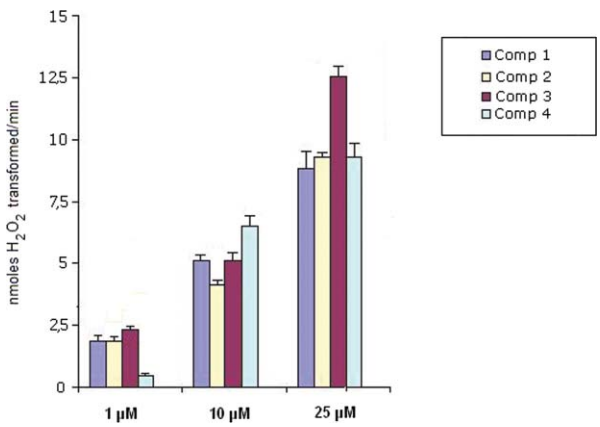

Fig. 10 Effects of synthesized compounds (1–25 μM) on the degradation of H_2O_2. Each bar represents the mean ± S.E.M. (indicated by vertical bars) for five experiments. Experiments were carried out in a total volume of 1 mL.

The K_{cat} values for all compounds were very similar and ranged between $7.49 \times 10^{-3} \pm 2.67 \times 10^{-4}$ s^{-1} and $2.67 \times 10^{-2} \pm 0.89 \times 10^{-3}$ s^{-1} (Table 6). In addition, the dimeric nickel(II) complex **3** was the most effective in degrading H_2O_2 since the corresponding K_{cat} value was significantly higher than the corresponding K_{cat} values for compounds **1**, **2** and **4**. Although these K_{cat} values were relatively low, the corresponding catalytic efficiency (K_{cat}/K_m) values were higher, as shown in Table 6. All of these kinetics correlated well with the Relative Catalase Activity (RCA), which was calculated for comparative purposes as indicated in the experimental part. The RCA values for all compounds were very close and ranged between 19.15 ± 0.86 μM and 27.70 ± 1.49 μM

Table 6 Parameters of catalase-like activity for **1–4** compounds

Complex	[comp] (μM)	$[H_2O_2]$ (μM)	V (nmoles H_2O_2 degraded/min)	V_{max} (nmoles H_2O_2 degraded/min)	K_{cat} $10^2(s^{-1})$	K_{cat}/K_m $(M^{-1}s^{-1})$	RCA (μM)
1	1	100	1.86 ± 0.19	14.71 ± 1.68	0.98 ± 0.07	169.46 ± 11.76	26.85 ± 0.97
	10	100	4.12 ± 0.62				
	25	100	9.29 ± 0.84				
	25	400	12.80 ± 0.75				
	25	25	3.32 ± 0.36				
2	1	100	1.86 ± 0.15	13.33 ± 0.86	0.89 ± 0.05	227.40 ± 6.34	27.70 ± 1.49
	10	100	5.11 ± 0.48				
	25	100	8.82 ± 0.62				
	25	400	13.22 ± 0.98				
	25	25	5.24 ± 0.44				
3	1	100	2.32 ± 0.06	40.00 ± 1.95	2.67 ± 0.09*	129.95 ± 4.52*	19.15 ± 0.86*
	10	100	5.21 ± 0.21				
	25	100	12.54 ± 0.64				
	25	400	28.08 ± 1.03				
	25	25	4.35 ± 0.05				
4	1	100	0.46 ± 0.12	11.24 ± 1.30	0.75 ± 0.03	367.32 ± 26.43	24.42 ± 1.27
	10	100	6.50 ± 0.74				
	25	100	9.27 ± 1.23				
	25	400	10.61 ± 0.98				
	25	25	7.96 ± 0.87				

Experiments were carried out in a total volume of 1 mL. Each value is the mean ± S.E.M. for five experiments. Level of statistical significance: $*P < 0.05$ with respect to the RCA, K_{cat} and K_{cat}/K_m values of the compounds **1**, **2** and **4**, as determined by ANOVA/Dunnett's.

(Table 6). In addition, the RCA value for compound **3** was slightly, but significantly, lower ($P < 0.05$) than the corresponding RCA values for compounds **1**, **2** and **4**, which indicates that compound **3** exhibits the highest catalytic activity.

Conclusion

The electrochemical oxidation of a metal anode (cobalt, nickel or copper) in a cell containing the potentially tetradentate Mannich base ligand allowed us to synthesize neutral complexes with high purities and good yields. The cobalt and copper complexes are dimeric with the metal atoms in a pentacoordinated environment whilst the crystal structure of the nickel complex shows the presence of a trimeric compound with the nickel atoms hexacoordinated. The presence of water in the cell allows the preparation of the dimer $[Ni_2L_2(H_2O)_{1.5}]\cdot CH_3CN$, in which the nickel is in both penta- and hexacoordinated environments. The weak antiferromagnetic interactions observed for the title compounds correlate quite well with their structural characteristics. The catalytic decomposition of H_2O_2 was also studied as a model reaction for catalase. All compounds showed catalytic activity, with the dimeric nickel(II) the most efficient.

Acknowledgements

This work was supported by the Ministerio de Ciencia y Tecnologia (Spain) (grants CTQ2006-05298 and CTQ 2007-64727-FEDER), Ministerio de Sanidad y Consumo (Spain; FISS PI061537) and by the Xunta de Galicia (Spain) (grants PGIDIT07PXIB-203038PR and PGIDIT05BTF20302PR).

References

1 G. J. P. Britovsek, V. C. Gibson and D. F. Wass, *Angew. Chem., Int. Ed.*, 1999, **38**, 428–447.
2 A. Van der Linden, C. J. Schaverien, N. Meijboom, C. Ganter and A. G. Orpen, *J. Am. Chem. Soc.*, 1995, **117**, 3008–3021.
3 (*a*) S. Fokken, T. P. Spaniol, H. C. Kang, W. Massa and J. Okuda, *Organometallics*, 1996, **15**, 5069–5072; (*b*) S. Fokken, T. P. Spaniol, J. Okuda, F. G. Sernetz and R. Mülhaupt, *Organometallics*, 1997, **16**, 4240–4242.
4 E. Y. Tshuva, M. Versano, I. Goldberg, M. Kol, H. Weitman and Z. Goldschmidt, *Inorg. Chem. Commun.*, 1999, **2**, 371–373.
5 (*a*) I. P. Rothwell, *Acc. Chem. Res.*, 1988, **21**, 153–159; (*b*) S. W. Schweiger, D. L. Tillison, M. G. Thorn, P. E. Fanwick and I. P. Rothwell, *J. Chem. Soc., Dalton Trans.*, 2001, 2401–2408.
6 D. E. Wigley, S. D. Gray, in *Comprehensive Organometallic Chemistry, III*, ed. E. W. Abel, F. G. Stone and G. Wilkinson, Pergamon Press, Oxford, England, 1995, vol. 5, pp. 57–153.
7 M. J. Caulfield, T. Russo and D. H. Solomon, *Aust. J. Chem.*, 2000, **53**, 545–549.
8 B. Castellano, E. Solari, C. Florián, N. Re, A. Chiesi-Villa and C. Rizzoli, *Chem.–Eur. J.*, 1999, **5**, 722–737.
9 L. Michalczyk, S. de Gala and J. W. Bruno, *Organometallics*, 2001, **20**, 5547–5556.
10 A. F. Kolodziej, in *Progress in Inorganic Chemistry*, ed. K. D. Karlin, Wiley, New York, 1994, pp. 494–597.
11 (*a*) J. A. Kovac, in *Advances in Inorganic Biochemistry*, ed. G. L. Eichorn and L. G. Marzilli. Prentice Hall, Englewood Cliffs, New Jersey, 1993, vol .9; (*b*) R. Commack, D. O. Hall, K. K. Rao in *Microbial gas metabolism mechanistic, metabolic and biotechnological aspects*, ed. R. K. Poole and C. S. Dow, Academic Press, London, England, 1985, p. 209; (*c*) G. Kubas, *Acc. Chem. Res.*, 1988, **21**, 120–128.
12 K. Yamaguchi, S. Koshino, F. Akag, M. Suzuki, A. Uehara and S. J. Suzuki, *J. Am. Chem. Soc.*, 1997, **119**, 5752–5753.
13 F. Zippel, F. Ahlers, R. Werner, W. Haase, H.-F. Nolting and B. Krebs, *Inorg. Chem.*, 1996, **35**, 3409–3419.
14 M. Tremolières and J. B. Bieth, *Phytochemistry*, 1984, **23**, 501–505.
15 C. A. Reed, R. D. Orosz, *Spin Coupling Concepts in Bioinorganic Chemistry*, ed. C. J. O'Connor, World Scientific, Singapore, 1993, pp. 351–393.

16 M. Melnik, M. Kabesová, M. Koman, L. Macáskova, J. Garaj, C. E. Holloway and C. E. Valent, *J. Coord. Chem.*, 1998, **45**, 147–359.
17 (*a*) K. D. Karlin, R. W. Cruse, Y. Gultneh, J. C. Hayes and J. Zubieta, *J. Am. Chem. Soc.*, 1984, **106**, 3372–3374; (*b*) T. N. Sorrell and M. L. Garrity, *Inorg. Chem.*, 1991, **30**, 210–215.
18 H. Diril, H.-R. Chang, X. Zhang, S. K. Larasen, J. A. Potenza, C. G. Pierpont, H. J. Schugar, S. S. Isied and D. N. Hendrickson, *J. Am. Chem. Soc.*, 1987, **109**, 6207–6208.
19 (*a*) M. Suzuki, H. Kanatomi and I. Murase, *Chem. Lett.*, 1981, 1745–1748; (*b*) M. Suzuki, I. Ueda, H. Kanatomi and I. Murase, *Chem. Lett.*, 1983, 185–188.
20 (*a*) H. Nie, S. M. J. Aubin, M. S. Mashuta, C.-H. Wu, J. F. Richardson, D. N. Hendrickson and R. M. Buchanan, *Inorg. Chem.*, 1995, **34**, 2382–2388; (*b*) S. Uhlenbrock and B. Krebs, B., *Angew. Chem., Int. Ed. Engl.*, 1992, **31**, 1647–1648.
21 (*a*) V. H. Crawford, H. W. Richardson, J. R. Wasson, D. J. Hodgson and W. E. Hatfield, *Inorg. Chem.*, 1976, **15**, 2107–2110; (*b*) D. J. Hodgson, *Prog. Inorg. Chem.*, 1975, **19**, 173–241; (*c*) A. Asokan, B. Varghese and P. T. Manoharan, *Inorg. Chem.*, 1999, **38**, 4393–4399; (*d*) K. Bertoncello, G. D. Fallon, J. H. Hodgkin and K. S. Murray, *Inorg. Chem.*, 1988, **27**, 4750–4758; (*e*) K. D. Karlin, A. Farooq, J. C. Hayes, B. I. Cohen, T. M. Rowe, E. Sinn and J. Zubieta, *Inorg. Chem.*, 1987, **26**, 1271–1280.
22 R. Gupta, S. Mukherjee and R. Mukherjee, *J. Chem. Soc., Dalton Trans.*, 1999, 4025–4030.
23 M. Zhou, Z. Diwu, N. Panchuk-Voloshina and R. P. Haugland, *Anal. Biochem.*, 1997, **253**, 162–168.
24 J. G. Mohanty, J. S. Jaffe, E. S. Schulman and D. G. Raible, *J. Immunol. Methods*, 1997, **202**, 133–141.
25 N. V. Timosheva, A. Chandrasckaran, R. O. Day and R. R. Holmes, *Inorg. Chem.*, 1998, **37**, 4945–4952.
26 E. Y. Tshuva, I. Golderg and M. Kol, *J. Am. Chem. Soc.*, 2000, **122**, 10706–10707.
27 (*a*) D. G. Tuck, *Pure Appl. Chem.*, 1979, **51**, 2005–2018; (*b*) M. C. Chakravorti and G. V. B. Subrahmanyam, *Coord. Chem. Rev.*, 1994, **135–136**, 65–92; (*c*) A. M. Vecchio-Sadus, *J. Appl. Electrochem.*, 1993, **23**, 401–416; (*d*) J. A. García-Vázquez, J. Romero and A. Sousa, *Coord. Chem. Rev.*, 1999, **193–195**, 691–745.
28 G. M. Sheldrick, *SADABS: Program for absorption correction using area detector data*, University of Göttingen, Göttingen, Germany, 1996.
29 G. M. Sheldrick, *SHELX97 [Includes SHELXS97, SHELXL97, CIFTAB]. Programs for Crystal Structure Analysis (Release 97-2)*, Institüt für Anorganische Chemie der Universität, Tammanstrasse 4, D-3400 Göttingen, Germany, 1998.
30 P. van der Sluis and A. L. Spek, *Acta Crystallogr., Sect. A: Found. Crystallogr.*, 1990, **46**, 194.
31 (*a*) A. L. Spek, *Acta Crystallogr., Sect. A: Found. Crystallogr.*, 1990, **46**, C43; (*b*) A. L. Spek, *PLATON, A Multiporpose Crystallographic Tool*, Utrecht University, Utrecht, The Netherlands, 1998.
32 L. J. Farrugia, ORTEP3 for Windows, *J. Appl. Crystallogr.*, 1997, **30**, 565.
33 (*a*) I. Beloso, J. Borrás, J. Castro, J. A. García-Vázquez, P. Pérez-Lourido, J. Romero and A. Sousa, *Eur. J. Inorg. Chem.*, 2004, 635–645; (*b*) J. Sanchez-Piso, J. A. García-Vázquez, J. Romero, M. L. Durán, A. Sousa-Pedrares, E. Labisbal and O. R. Nascimento, *Inorg. Chim. Acta*, 2002, **328**, 111–112; (*c*) A. D. Garnovskii, A. S. Bulov, D. A. Garnovskii, I. S. Vasilchenkkop, A. S. Antsichkina, G. G. Sadikov, A. Sousa, J. A. García-Vázquez, J. Romero, M. L. Durán, A. Sousa-Pedrares and C. Gómez, *Polyhedron*, 1999, **18**, 863–869; (*d*) J. Castro, J. Romero, J. A. García-Vázquez, A. Castiñeiras, M. L. Durán and A. Sousa, *Z. Anorg. Allg. Chem.*, 1992, **615**, 155–160.
34 A. W. Addison, T. N. Rao, J. Reedjijk, J. van Rijn and G. C. Verschoor, *J. Chem. Soc., Dalton Trans.*, 1984, 1349–1356.
35 M. Du, D. L. An, Y. M. Guo and X. H. Bu, *J. Mol. Struct.*, 2002, **641**, 193–198.
36 H. Furutachi and H. Okawa, *Inorg. Chem.*, 1997, **36**, 3911–3918.
37 R. Cini, *Acta Crystallogr., Sect. C: Cryst. Struct. Commun.*, 2001, **C57**, 1171–1173.
38 (*a*) L. Rodríguez, E. Labisbal, A. Sousa-Pedrares, J. A. García-Vázquez, J. Romero, M. L. Durán, J. A. Real and A. Sousa, *Inorg. Chem.*, 2006, **45**, 7903–7914; (*b*) S. Kita, H. H. Furutachi and H. Okawa, *Inorg. Chem.*, 1999, **38**, 4038–4045.
39 R. Boca, H. G. Elias, W. Haase, M. Huber, R. Klement, L. Muller, H. Paulus, I. Svoboda and M. Valko, *Inorg. Chim. Acta*, 1998, **278**, 127–135.
40 (*a*) S. C. Telfer and R. Kurodo, *Chem.–Eur. J.*, 2005, **11**, 57–68; (*b*) S. C. Telfer, T. Soto and R. Kuroda, *Angew. Chem., Int. Ed.*, 2004, **43**, 581–584; (*c*) K. J. Tubbs, E. Szajna, B. Bennett, J. A. Halfeu, R. W. Walkins, A. M. Arif and L. M. Berreau, *Dalton Trans.*, 2004, 2398–2399; (*d*) C. Incarvito, A. L. Rheingold, C. Jin Qin, A. L. Gavrilova and B. Bosnich, *Inorg. Chem.*, 2001, **40**, 1386–1390.
41 G. Bertier, J. Serre, *The chemistry of the Carbonyl Group*, ed. S. Patai, Interscience, New York, 1966.
42 E. V. Rybak-Akimova, N. W. Alcock and D. H. Busch, *Inorg. Chem.*, 1998, **37**, 1563–1574.
43 H. Luo, J.-M. Lo, P. E. Fanwick, J. G. Stowell and M. A. Green, *Inorg. Chem.*, 1999, **38**, 2071–2078.
44 S. Mohanta, K. K. Namda, R. Werner, W. Haase, A. K. Mukherjee, S. H. Dutta and K. K. Nag, *Inorg. Chem.*, 1997, **36**, 4656–4664.
45 H. Adams, S. Clunas, D. E. Fenton, E. David;, T. J. Gregson;, P. E. McHugh; and S. E. Spey, *Inorg. Chim. Acta*, 2003, **346**, 239–247.
46 D. Kong, X. Ouyang, J. Relbenspies, A. Clearfield and A. E. Martell, *Inorg. Chem. Commun.*, 2002, **5**, 873–878.
47 K. K. Nanda, K. Venkatsubramanian, D. Majundar and K. Nag, *Inorg. Chem.*, 1994, **33**, 1581–158.
48 H. Adams, S. Clunas and D. E. Fenton, *Inorg. Chem. Commun.*, 2001, **4**, 667–670.
49 K. K. Nanda, R. Das, L. K. Thompson, K. Venkatsubramanian, P. Paul and K. Nag, *Inorg. Chem.*, 1994, **33**, 1188–1193.
50 H. Adams, D. E. Fenton, L. R. Cummings, P. E. McHugh, M. Ohba, H. Okawa, H. Sakiyama and T. Shiga, *Inorg. Chim. Acta*, 2004, **357**, 3648–3656.
51 S. J. Kirin, C. M. Happel, S. Hrubanova, T. Weyhermüller Klein and N. Metzler-Nolte, *Dalton Trans.*, 2004, 1201–1207.
52 J. Cho, H. Futachi, S. Fujinami and M. Suzuki, *Angew. Chem., Int. Ed.*, 2004, **43**, 3300–3303.
53 K. Rudzka, M. M. Makowska-Crzyska, E. Szajna, A. M. Arif and L. M. Rerreau, *Chem. Commun.*, 2005, 489–491.
54 (*a*) Y. Shimazaki, S. Huth, S. Karasawa, S. Hirota, Y. Naruta and O. Yamauchi, *Inorg. Chem.*, 2004, **43**, 7816; (*b*) H. Ohtsu and K. Tanaka, *Inorg. Chem.*, 2004, **43**, 3024–3030.
55 (*a*) X. H. Bu, M. Du, L. Zhang, Z. L. Shang, R. H. Zang and H. Shionoya, *J. Chem. Soc., Dalton Trans.*, 2001, 729–735; (*b*) M. Vaidyanathan, M. Palaniandavar and R. S. Gopalan, *Inorg. Chim. Acta*, 2001, **324**, 241–251; (*c*) D. Kong, J. Mao, A. E. Martell and A. Clearfield, *Inorg. Chim. Acta*, 2003, **342**, 260–266.
56 O. Kahn, *Molecular Magnetism*, VCH, New York, 1993.
57 A. P. Ginsberg, R. L. Martin, R. W. Brookes and R. C. Sherwood, *Inorg. Chem.*, 1972, **11**, 2884–2889.
58 (*a*) A. P. Ginsberg, R. L. Martin and R. C. Sherwood, *Inorg. Chem.*, 1968, **7**, 932–936; (*b*) U. Auerbach, C. Stockheim, T. Weyhemuller, K. Wieghardt and B. Nuber, *Angew. Chem., Int. Ed. Engl.*, 1993, **32**, 714–716; (*c*) T. Beissel, T. Glaser, F. Kesting, K. Wieghardt and B. Nuber, *Inorg. Chem.*, 1996, **35**, 3936–3947; (*d*) J. M. Clemente-Juan, E. Coronado, J. R. Galán-Mascarós and C. J. Gómez-García, *Inorg. Chem.*, 1999, **38**, 55–63; (*e*) H. Ohta, K. Harada, K. Irie, S. Kashino, T. Kambe, G. Sakane, T. Shibahara, S. Takamizawa, W. Mori, M. Nonoyama, M. Hirotsu and M. Kojima, *Chem. Lett.*, 2001, 842–843; (*f*) V. Chandrasekhar, R. Azhakar, G. T. S. Andavan, V. Krishnan, S. Zacchini, J. F. Bickley, A. Steiner, R. J. Butcher and P. Kögerler, *Inorg. Chem.*, 2003, **42**, 5989–5998.
59 X.-H. Bu, M. Du, L. Zhang, D.-Z. Liao, J.-K. Tang, R.-H. Zhang and M. Shionoya, *J. Chem. Soc., Dalton Trans.*, 2001, 593–598.
60 J. Kaizer, G. Barath, G. Speier, M. Réglier and M. Grigori, *Inorg. Chem. Commun.*, 2007, **10**, 292–294.
61 A. Gelasco, S. Bensiek and V. L. Percoraro, *Inorg. Chem.*, 1998, **37**, 3301–3309.
62 J. Kaizer, T. Casay, G. Speier, M. Réglier and M. Giorgi, *Inorg. Chem. Commun.*, 2006, **9**, 1037–1039.
63 S. Signorella, A. Rompel, K. Buld-Karetzopoulos, B. Krebs, V. L. Percoraro and J.-P. Tuchagues, *Inorg. Chem.*, 2007, **46**, 10864–10868 and references therein.